# Effects of Water Vapor and Trace Gas Impurities in Flue Gas on CO2/N2 Separation Using ZIF-68

**4 AUTHORS**, INCLUDING:

Yang Liu
King Abdula university of science and technol...
**5** PUBLICATIONS **55** CITATIONS

SEE PROFILE

Jing Liu
Huazhong University of Science and Technology
**40** PUBLICATIONS **603** CITATIONS

SEE PROFILE

Jerry Y S Lin
Arizona State University
**307** PUBLICATIONS **9,520** CITATIONS

SEE PROFILE

# Effects of Water Vapor and Trace Gas Impurities in Flue Gas on CO$_2$/N$_2$ Separation Using ZIF-68

Yang Liu,[†,‡] Jing Liu,*[,†] Y.S. Lin,[‡] and Ming Chang[§]

[†]State Key Laboratory of Coal Combustion, Huazhong University of Science and Technology, Wuhan 430074, China
[‡]School for Engineering of Matter, Transport and Energy, Arizona State University, Tempe, Arizona 85287-6006, United States
[§]School of Materials Science and Engineering, Wuhan University of Technology, Wuhan 430070, China

Ⓢ *Supporting Information*

**ABSTRACT:** Understanding the effects of the presence of water vapor and other gas impurities (such as SO$_2$ and O$_2$) in flue gas on sorbent performance is critical to properly evaluate the use of metal organic frameworks for realistic postcombustion CO$_2$ capture. Grand canonical Monte Carlo calculations were performed to investigate the effects of H$_2$O, O$_2$, and SO$_2$ on CO$_2$ adsorption and CO$_2$/N$_2$ separation using ZIF-68. The mechanisms of these effects were also investigated by density functional theory calculations. The presence of H$_2$O affects the CO$_2$ adsorption on ZIF-68 in two opposite ways: the negative effect of competitive adsorption of the impurity gases on the adsorption sites over CO$_2$, and the positive effects of formation of new adsorption sites for CO$_2$. The presence of H$_2$O reduces the CO$_2$ adsorption ability but increases the CO$_2$/N$_2$ separation factor. SO$_2$ is found to be strongly adsorbed in the pores of ZIF-68 and considered as an adverse factor for CO$_2$ adsorption and CO$_2$/N$_2$ separation. The presence of O$_2$ has a negligible effect on CO$_2$ adsorption on ZIF-68.
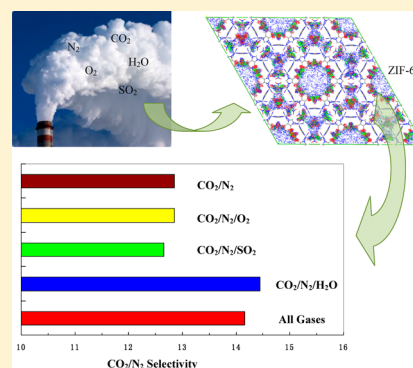
## 1. INTRODUCTION

Capturing CO$_2$ from flue gases using porous materials is one of the promising approaches for CO$_2$ capture and sequestration.[1] Recently, many new synthetic and natural organic porous materials have been studied for this purpose. Among these materials, metal organic frameworks (MOFs) show great potential.[2−4] One of the advantages of MOFs is the ability to modulate systematically the pore dimensions and surface chemistry within their framework, allowing tailoring sorbent materials for effective CO$_2$ capture.[5] Zeolitic imidazolate frameworks (ZIFs) constitute a subclass of MOFs that adopt zeolite structure types.[6,7] In contrast to many MOF materials, ZIFs have better thermal and chemical stability more suitable for practical CO$_2$ capture applications.[8]

Most studies on ZIF sorbents were focused on the CO$_2$ adsorption capacity and CO$_2$/N$_2$ adsorption selectivity to evaluate the potential uses of these materials for postcombustion CO$_2$ capture.[6,9−11] Banerjee et al.[6] first reported the extraordinary capacity of ZIFs for storing CO$_2$: 1 L of ZIF-69 can hold 83 L of CO$_2$ at 273 K under ambient pressure. They also investigated the functionality effects on CO$_2$ uptake capacity in an isoreticular series of ZIFs with similar GME topology but different functional groups.[9] Calculations of breakthrough curves indicate that ZIFs have much higher selectivity for CO$_2$ in CO$_2$/N$_2$ gas mixtures than the industrially pertinent BPL carbon.[9] Recently, grand canonical Monte Carlo (GCMC) calculations have also been performed to investigate the adsorption or separation behaviors of CO$_2$ in ZIF materials.[12−16] Liu et al.[12] reproduced the experimental CO$_2$

adsorption isotherms in ZIF-68 and ZIF-69 very well by GCMC calculations using classic UFF force field. They also found that the small pores formed by the nIM linkers are the preferential adsorption sites for CO$_2$ molecules,[12] which is difficult to be observed by experimental methods. Liu and Smit[13] evaluated the separation performance of ZIF-68 and ZIF-69 for CO$_2$/N$_2$, CO$_2$/CH$_4$, and CH$_4$/N$_2$ mixtures using a similar force field. Besides the GCMC method, density functional theory (DFT) is also widely used as an important means to study the mechanism of CO$_2$ adsorption in ZIFs. In our previous work, DFT calculations were performed to investigate the effects of functionalized linkers on CO$_2$ binding in ZIFs, which is helpful to design new ZIF materials with higher CO$_2$ adsorption ability.[17] However, although it is valuable to investigate the various influence factors on the CO$_2$ adsorption and separation performance of ZIFs and then find effectual ways to improve these abilities, the investigations on the effect of the operation conditions should also be performed in order to evaluate the potential of ZIFs using in a realistic industrial system.

It is well known that flue gas for coal-fired power plants contains roughly about 73−77% N$_2$, 15−16% CO$_2$, 5−7% H$_2$O, 3−4% O$_2$, and trace amounts of impurities such as SO$_2$.[18,19] Although many works were conducted to investigate the effects of water vapor on CO$_2$ adsorption or CO$_2$/N$_2$ separation

properties of MOFs,[20−24] only a few studies have been performed in the area of ZIFs.[13,25] Liu and Smit[13] reported that the presence of water vapor (less than 5%) has negligible effects on $CO_2$ adsorption properties of ZIF-68 by GCMC works. Huang et al.[25] found that the interaction between water molecules and the framework plays a crucial role when evaluating the effect of a trace amount of water on $CO_2$ capture in the natural gas upgrading process in MOFs and ZIFs. However, the mechanism of these interactions is still not clear. Besides the effect of water, $SO_2$ was also considered as a significant threat to $CO_2$ capture in porous materials.[26−28] Up to date, limited knowledge is available on the $SO_2$ adsorption in ZIFs. Ding and Yazaydin[29] investigated the $CO_2$ capture performance of four ZIF materials in the presence of $SO_2$ using molecular simulations and found a cooperative interaction between $SO_2$ and $CO_2$ molecules. Explaining the cobinding mechanism of $CO_2$ and $H_2O$ or $SO_2$ in ZIFs by a more accurate quantum chemical method is expected to be helpful to understand the effect of $H_2O$ or $SO_2$ presence on $CO_2$ adsorption in ZIFs.

ZIF-68 is one of representative ZIF materials with good $CO_2$ adsorption and $CO_2/N_2$ separation characteristics.[5,6,8] In the present work, the GCMC method was used to predict the effects of water vapor and other trace gas impurities ($O_2$ and $SO_2$) on $CO_2/N_2$ separation properties of ZIF-68. The mechanisms of these influences were thoroughly investigated by GCMC and DFT calculations. To the best of our knowledge, this is the first work to explore the binding mechanism of $H_2O$ and $SO_2$ on ZIFs as well as the cointeraction mechanisms between $CO_2$ and $H_2O$ or $SO_2$ on ZIFs.

## 2. COMPUTATIONAL METHODOLOGY

**2.1. ZIF Structure.** ZIF-68 has typically GME zeolite-type topology with Zn connected to benzimidazole (bIM) and 2-nitroimidazole (nIM) to create a corresponding tetrahedron. The ZIF-68 structure was constructed from experimental X-ray diffraction (XRD) data,[6] and the atoms belonging to the residual solvent molecules were removed. The experimental crystal structure was directly used in our simulations without DFT optimization.

**2.2. Force Field.** The interaction of gas−adsorbent and gas−gas were modeled as a combination of site−site Lennard−Jones (LJ) and Coulombic potentials:

$$u_{ij}(r) = \sum_{\substack{\alpha \in i \\ \beta \in j}} \left\{ 4\varepsilon_{\alpha\beta} \left[ \left( \frac{\sigma_{\alpha\beta}}{\gamma_{\alpha\beta}} \right)^{12} - \left( \frac{\sigma_{\alpha\beta}}{\gamma_{\alpha\beta}} \right)^{6} \right] + \frac{q_\alpha q_\beta}{4\pi\varepsilon_0 \gamma_{\alpha\beta}} \right\} \quad (1)$$

where $\varepsilon_0$ equals $8.8542 \times 10^{-12}$ $C^2$ $N^{-1}$ $m^{-2}$ and is the permittivity of the vacuum, and $\sigma_{\alpha\beta}$ and $\varepsilon_{\alpha\beta}$ are the collision diameter and well depth, respectively. UFF force field[30,31] has successfully been used by Liu et al.[12] and Sirjoosingh et al.[15] to describe the $CO_2$ adsorption isotherm in ZIF-68 and therefore is used in this work. The partial charges of the framework atoms (as shown in the Supporting Information) obtained using Mulliken charge partitioning method by Liu et al.[12] are used to model the charge interactions between the framework atoms and the gas molecules. The spherical united-atom LJ potential model was used to represent $N_2$ and $O_2$.[32] $CO_2$, $SO_2$, and $H_2O$ were modeled as a three sites rigid linear molecule with quadrupole moment described by a partial charge model.[33]

Lorentz−Berthelot mixing rules were used to determine the LJ cross-interaction parameters.[34] All of the LJ potential parameters and atomic charges used in this work are listed in the Supporting Information.

**2.3. Details of GCMC Calculations.** The conventional GCMC method was used to investigate the adsorption and separation of various gases in ZIF-68. The ZIF-68 framework was treated as rigid with atoms frozen at their crystallographic positions during GCMC simulations. A simulation box containing 8 ($2 \times 2 \times 2$) unit cells with periodic boundary conditions applied in all three dimensions was built in this work. A cutoff radius was set to 12.8 Å for the LJ interactions, and the long-range electrostatic interactions were handled using the Ewald summation method with the tinfoil boundary condition. For each state point, GCMC simulation consists of $1.0 \times 10^7$ steps to guarantee the equilibration, followed by $1.0 \times 10^7$ steps to sample the desired thermodynamics properties. The GCMC calculations were performed using the Sorption code in Materials Studio 4.4.[35] The selectivity for component A relative to component B is defined by the following: $S = (\alpha_A/\alpha_B)(\beta_B/\beta_A)$, where $\alpha$ and $\beta$ are the molar fractions of components A and B in the adsorbed and gas phases, respectively.

**2.4. Details of DFT Calculations.** Cluster models were constructed using the method as described in our previous study.[17,36] All of the theoretical calculations were performed by DFT method using the Dmol[3] code in Materials Studio 4.4.[35,37] The DFT method in this code uses fast convergent three-dimensional numerical integration to calculate the necessary matrix elements, and it is also an efficient and exact method for calculating the electrostatic potential. The PW91 exchange-correlation functional,[38] which is considered adequate with quantitative precision for the investigation of weak van der Waals force between MOFs and $CO_2$,[39] was used in the current work. The double numeric polarization (DNP)[37] basis set, which is comparable to 6-31G(d,p), was used to describe the atomic orbital. DFT Semicore Pseudopots (DSPP)[40] that is developed specifically for DMol[3] calculations was used to set the type of core treatment.

Both of the initial cluster models (fragment 1 and fragment 2), as shown in the Supporting Information, were first optimized using the calculation methods described above. After the geometry optimizations, gas molecules were placed in different configurations separately. Additional geometry optimizations were performed to every configuration, and the binding energies were calculated. The binding energy (BE) of an adsorbate "A" on a substrate "B" can be calculated as follows:

$$BE = E(AB) - (E(A) + E(B)) \quad (2)$$

where $E(A)$ is the total energy of the adsorbate, $E(B)$ is the total energy of the substrate, and $E(AB)$ is the total energy of the adsorbate/substrate system in the equilibrium state. Binding of the adsorbate is exothermic if BE is negative. A higher negative value of BE corresponds to a stronger binding.

## 3. RESULTS AND DISCUSSION

**3.1. Sorption of Pure Gases on ZIF-68.** In a previous work, Liu et al.[12] validated the reliability of using the similar classical UFF parameters and atomic charges to describe $CO_2$ adsorption in ZIF-68. The bulk PVT behavior of $CO_2$ gas at different temperatures was calculated using NPT MC simulations to validate the force field for $CO_2$. In this work,

the reliability of the GCMC calculation was also validated by comparing the simulation data with experimental adsorption isotherms of $CO_2$, $N_2$, and $O_2$ in ZIF-68,[9] which is available in the Supporting Information. From the comparison, the parameters used in this work give good reproduction of the corresponding experimental adsorption isotherms, which validates that the force fields used in this work are applicable.

Figure 1 shows the pure gas sorption isotherm of $N_2$, $CO_2$, $O_2$, $H_2O$, and $SO_2$ in ZIF-68 as a function of pressures. The
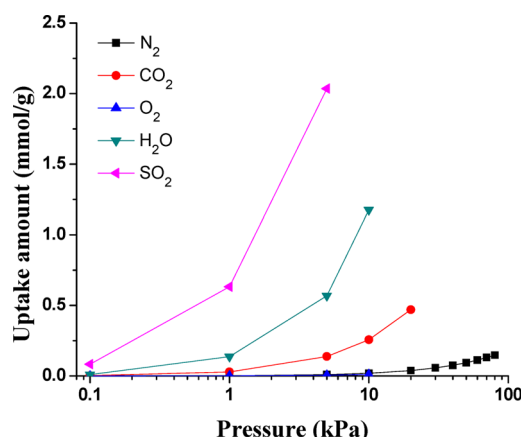


**Figure 1.** Pure gas sorption isotherm of various gases ($N_2$, $CO_2$, $O_2$, and $SO_2$) and $H_2O$ in ZIF-68 at 298 K and the pressures in range of the partial pressures of the components in flue gas ($N_2$: 0−80 kPa; $CO_2$: 0−20 kPa; $O_2$: 0−10 kPa; $H_2O$: 0−10 kPa; $SO_2$: 0−5 kPa). The saturation pressure is 3.16 kPa for water.

partial pressures of $N_2$, $CO_2$, $O_2$, $H_2O$, and $SO_2$ in flue gas are used for different components. As shown in Figure 1, the uptake amount of $CO_2$ in ZIF-68 is significantly higher than that of $N_2$, which indicates that ZIF-68 is a good material for $CO_2/N_2$ separation. The uptake amount of $O_2$ in ZIF-68 is quite low. It is notable that the uptake amount of $SO_2$ and $H_2O$ are very high even at low pressure, which means there is a strong interaction between them and and the ZIF-68 framework. In order to quantitatively compare the uptakes of various gases in ZIF-68, the uptake amount and isosteric heat of them at 1 kPa were illustrated in Table 1.

**Table 1. Uptake Amount and Isosteric Heat of Various Gases ($N_2$, $CO_2$, $O_2$, $H_2O$, and $SO_2$) in ZIF-68 at 298 K and 1 kPa**

|  | $N_2$ | $CO_2$ | $O_2$ | $H_2O$ | $SO_2$ |
|---|---|---|---|---|---|
| uptake amount | 0.002 | 0.029 | 0.001 | 0.136 | 0.632 |
| isosteric heat | 13.0 | 23.0 | 11.4 | 32.8 | 37.0 |

Table 1 shows the uptake amount of various gases in ZIF-68 at 1 kPa and 298K, which varies widely in the sequence of $SO_2$ > $H_2O$ > $CO_2$ > $N_2$ > $O_2$. Correspondingly, the isosteric heat of these gases follows the same trend. It is notable that $SO_2$ and $H_2O$ have much higher uptake capacity than $CO_2$ in ZIF-68 at the given pressure. In previous studies, $SO_2$ was also found to be adsorbed in larger amounts than $CO_2$ in several different MOFs with open metal sites or amine groups.[26]

The spatial probability distributions of $H_2O$, $CO_2$, and $SO_2$ in ZIF-68 at 298 K and 1 kPa are also shown in Figure 2a−c, respectively. From Figure 2a, $H_2O$ sorption is mainly observed in the small pores. However, $CO_2$ adsorption in both pores and
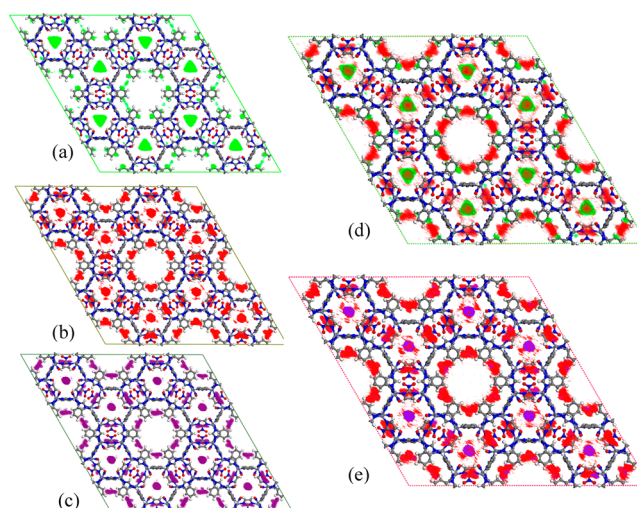


**Figure 2.** Probability distribution for (a) $H_2O$ (green dots), (b) $CO_2$ (red dots), (c) $SO_2$ (purple dots), and their mixtures (d) $CO_2/H_2O$ and (e) $CO_2/SO_2$ with an equal molar ratio (1:1) at 298 K and a total pressure of 1 kPa.

channels is seen (Figure 2b). The distribution of $SO_2$ in ZIF-68 is very similar to that of $CO_2$ but is more concentrated (Figure 2c). These phenomena are due to the differential of the nature of interaction forces between ZIF-68 and various gas molecules as well as the different gas molecular diameters. In a previous study, Liu et al.[12] reported that the small pores formed by the nIM linkers are the preferential sites for $CO_2$ adsorption in ZIF-68 and with increasing pressure $CO_2$ molecules were first adsorbed in the corners formed by the phenyl rings in the large pores and then occupied the center of the pores. Here, our GCMC calculations show that the small pores are also the preferential sites for $SO_2$ and $H_2O$ molecules, which may affect the $CO_2$ adsorption behavior a lot because competitive adsorption between them and $CO_2$ molecules may occur during the adsorption process.

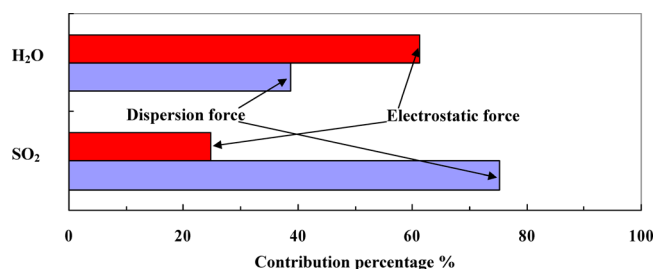Figure 3 shows the contribution percentage of dispersion force and electrostatic force to $SO_2$ and $H_2O$ uptake at 1 kPa.



**Figure 3.** Contribution percentage of electrostatic force (red) and dispersion force (blue) to $SO_2$ and $H_2O$ uptake amount in ZIF-68 at 1 kPa.

The substantial effect of $H_2O$ is largely attributed to the electrostatic interactions because $H_2O$ molecules are highly polar molecules, while dispersion forces play a relative weaker role during this process. In the case of $SO_2$, although electrostatic force is also significant, the role of dispersion force is still the dominant force (Figure 3). Additional GCMC simulations were also performed for $SO_2$ and $H_2O$ uptakes in ZIF-68 by switching off the charges of adsorbed molecules and/or framework atoms, which is available in the Supporting
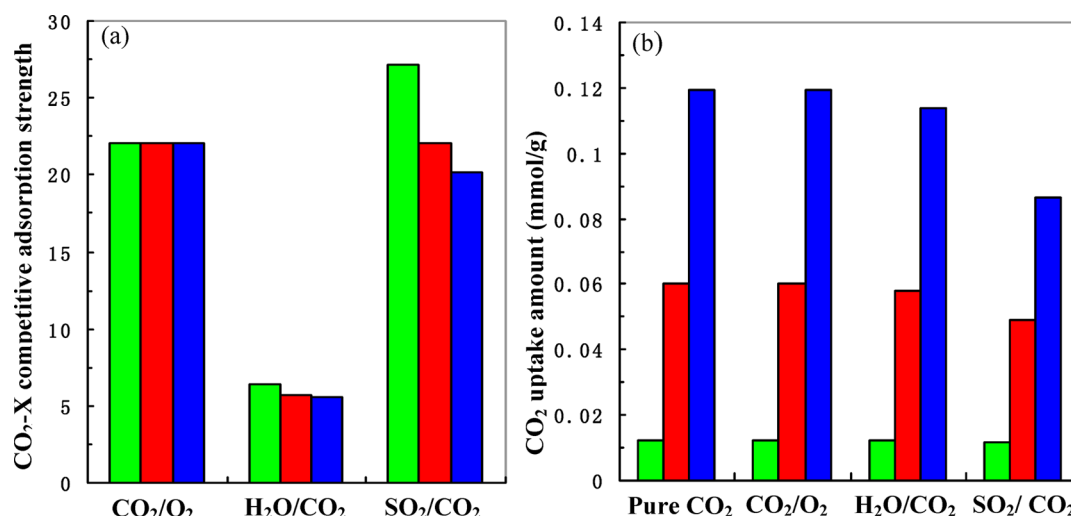
**Figure 4.** (a) Selectivity of $CO_2$ from $CO_2/O_2$, $H_2O$ from $H_2O/CO_2$, and $SO_2$ from $SO_2/CO_2$; (b) $CO_2$ uptake amount in mixtures with equal molar ratio (1:1) at 1 kPa (green), 5 kPa (red), and 10 kPa (blue).

Information. The results show that the contribution of atomic charges to the $SO_2$ and $H_2O$ uptake amount is significant.

**3.2. Selectivity of Binary Mixtures.** The cobinding of binary mixtures ($CO_2/O_2$, $H_2O/CO_2$, and $SO_2/CO_2$) in ZIF-68 was investigated. Figure 4a shows the selectivity of $CO_2/O_2$, $H_2O/CO_2$, and $SO_2/CO_2$ with equal molar ratio (1:1) at 1, 5, and 10 kPa, respectively. It can be seen that ZIF-68 shows pretty good selectivity for $CO_2$ from $CO_2/O_2$ mixtures, which indicates $CO_2$ is preferentially adsorbed over $O_2$ (Figure 4a). In addition, the $CO_2$ uptake amount in the $CO_2/O_2$ mixture does not change comparing to the data obtained from the pure gas uptake measurements (Figure 4b). Thus $O_2$ is considered to hardly influence the $CO_2$ adsorption in ZIF-68, which is similar with the results obtained in previous work where MOF materials with open metal sites or amine group were used.[26]

ZIF-68 prefers $H_2O$ to $CO_2$ in the $H_2O/CO_2$ mixture (Figure 4a). Figure 2d provides the spatial probability distributions of $CO_2$ and $H_2O$ cobinding in ZIF-68 at 1 kPa. Due to the fact that the small pores are the most favorite adsorption sites for both $CO_2$ and $H_2O$ molecules, they compete with each other in the small pores for the limited positions at such low pressure. For $CO_2$ and $SO_2$ cobinding in ZIF-68, the selectivity for $SO_2$ from $CO_2$ is even higher than that of $H_2O$ from $CO_2$ due to the stronger interaction force (Figure 4a). In Figure 2e, one can see that $SO_2$ molecules almost occupy all the position of small pores and $CO_2$ molecules briefly appear at the other sites, which is similar with the cobinding of $CO_2$ and $SO_2$ in HKUST-1.[26] The uptake amount of $CO_2$ is not affected by $H_2O$ or $SO_2$ at low pressure (total pressure 1 kPa) owing to plenty of adsorption sites for gas molecules to occupy but is significantly affected by $SO_2$ and $H_2O$ when the total pressure increases to 5 and 10 kPa, as shown in Figure 4b. A decrease of the selectivity for $H_2O$ or $SO_2$ from $CO_2$ is observed when the pressure increase from 1 to 10 kPa, while the selectivity for $CO_2$ from $O_2$ is almost maintained (Figure 4a). In a word, both of $H_2O$ and $SO_2$ have negative effect to $CO_2$ adsorption in ZIF-68.

**3.3. Effects of $O_2$, $H_2O$, and $SO_2$ on $CO_2/N_2$ Selectivity.** The selectivity for $CO_2$ from a binary mixture of $CO_2/N_2$ with a 16%:84% partial pressure ratio was calculated and is available in the Supporting Information. We can see that $CO_2$ is preferentially adsorbed over $N_2$, which makes ZIF-68 a good

choice for $CO_2/N_2$ separation application. In real $CO_2$ capture applications, a high selectivity for $CO_2$ from a $CO_2/N_2$ mixture in the presence of impurities is essential. In order to study the effect of $O_2$, $H_2O$, and $SO_2$ on $CO_2/N_2$ separation in ZIF-68, four different gas mixtures were considered: (1) $CO_2/N_2/O_2$, (2) $CO_2/N_2/SO_2$, (3) $CO_2/N_2/H_2O$, and (4) $CO_2/N_2/O_2/SO_2/H_2O$. Partial pressures of each gas were defined to simulate the real composition of each in flue gases: 16 kPa for $CO_2$, 4 kPa for $O_2$, 3.16 kPa for $H_2O$, and 0.08 kPa for $SO_2$. $N_2$ was used to balance the total pressure in the mixtures. The total pressure of the simulated flue gas is 100 kPa. Figure 5 shows the obtained $CO_2/N_2$ selectivity of all cases and the corresponding uptake amount of $CO_2$ and $N_2$.

As shown in Figure 5a, the injection of $O_2$ into $CO_2/N_2$ (mixture $CO_2/N_2/O_2$) does not change the $CO_2/N_2$ separation factor as well as the uptake amounts of $CO_2$ and $N_2$. On the
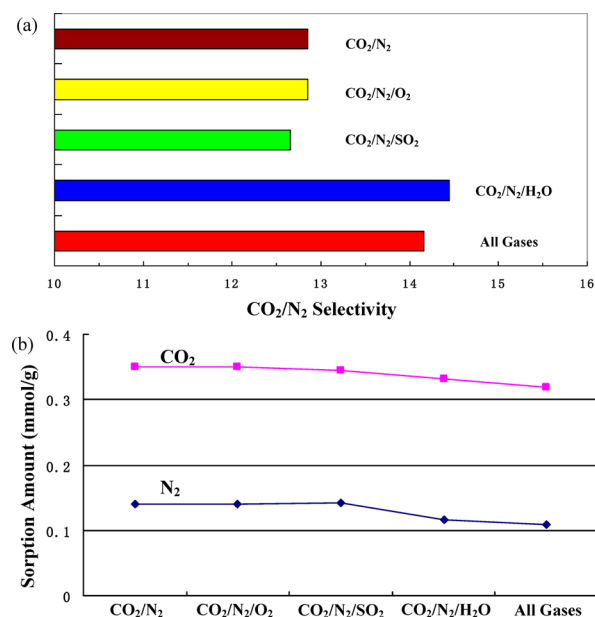


**Figure 5.** (a) $CO_2/N_2$ selectivity and (b) $CO_2$ and $N_2$ uptake amount in the mixtures of $CO_2/N_2$, $CO_2/N_2/O_2$, $CO_2/N_2/SO_2$, $CO_2/N_2/H_2O$, and all gases ($CO_2/N_2/O_2/SO_2/H_2O$) at 298 K and 100 kPa.

other hand, after adding 800 ppm $SO_2$ (mixture $CO_2/N_2/SO_2$), the $CO_2/N_2$ selectivity and the $CO_2$ uptake amount decrease slightly, but the $N_2$ uptake amount does not change (Figure 5b). However, the $CO_2/N_2$ selectivity is significantly improved in the presence of $H_2O$ (Figure 5a). Both the $CO_2$ and $N_2$ uptake amount decrease in this process, but the decrement of $N_2$ is larger than that of $CO_2$ (Figure 5b). The reasons can be explained as follows: (1) the partial pressure of $N_2$ is significantly decreased; and (2) besides the negative effect of $H_2O$ on $CO_2$ adsorption, there is also a kind of positive effect to counteract part of the negative effect, but this positive effect is absence on $N_2$ adsorption. In the mixture $CO_2/N_2/O_2/H_2O/SO_2$, the value of $CO_2/N_2$ selectivity is moderate because of the coexistence of $SO_2$ and $H_2O$.

**3.4. Mechanism.** GCMC results discussed above provide generic information of gas impurities uptake in ZIF-68. In the following discussion, specific information of the interaction mechanisms obtained from DFT calculations is presented and discussed. Two different fragments were constructed to present the IM linker and the nIM linker, as illustrated in the Supporting Information. It should be noted that using simplified fragments may not accurately describe the electrostatic environment inside the pores of porous material but can give specific information when discussing the variety of interaction mechanisms between the organic linkers composing the pores and various gas molecules.[17] Several studies used a similar termination method to give a qualitative discussion of the gas interaction mechanism in MOFs.[41,42] Besides, the DFT method used here is within acceptable errors for obtaining binding energies compared to the MP2 method and provides a good balance between accuracy and computational cost. Torrisi et al.[41] reported that the absolute values of the BEs, which are calculated by the DFT-PW91 functional and a double numerical plus (DNP) polarization basis set, are in good agreement with the BEs calculated by the MP2 method when using a triple $\zeta$, Pople basis set plus diffuse function. They also compared the BEs and geometries of the benzene/$CO_2$ molecular complex calculated by DFT and MP2 methods and found that the closest BE and the closest $C(CO_2)$-CM (center of mass) distance can be given by the PW91/DNP method of DFT to the MP2/6-311+G(2d,2p) values.[44] The DFT method has been extensively used to investigate the $CO_2$[41−43] and $H_2$[44−47] adsorption in MOFs, where the dominant force is van der Waals forces.

Several stable configurations of $CO_2$, $SO_2$, and $H_2O$ on the fragments of ZIF-68 are shown in the Supporting Information. The highest BEs for each site are selected and illustrated in Table 2. Obviously, in the case of $H_2O$ and $CO_2$, the BEs follow

**Table 2. Highest Binding Energy (kJ/mol) of $CO_2$, $SO_2$, or $H_2O$ on Fragments of ZIF-68 Obtained from DFT Calculations**

|  | $CO_2$ | $H_2O$ | $SO_2$ |
|---|---|---|---|
| fragment 1 | −9.1 | −17.7 | −51.9 |
| fragment 2 | −13.1 | −35.1 | −18.7 |

the same trend for both fragments: $H_2O > CO_2$, and the BEs of fragment 2 are larger than those of fragment 1. This can be attributed to the fact that (1) $H_2O$ is a polar molecule and thus has much stronger interactions with the adsorbent than $CO_2$ with quadrupolar moments and (2) the polar functional group −$NO_2$ can enhance the interactions between the adsorbent and

$H_2O$ or $CO_2$. Meanwhile, considering that fragments 1 and 2 are the major components to construct the large pores and small pores, respectively, the small pores with much larger BEs for gas molecules are the preferential sorption sites for $H_2O$ and $CO_2$, which is in good agreement with our GCMC results.

Unlikely $H_2O$ and $CO_2$, BEs of $SO_2$ molecules on fragment 1 are much larger than those on fragment 2 (Table 2). The BE is −51.9 kJ/mol, which indicates a strong interaction between the $SO_2$ molecule and fragment 1. The Mulliken atomic charges of the stable configurations for $SO_2$ and fragments 1 and 2 were also calculated and shown in the Supporting Information. The results show that large charge transferring occurred between $SO_2$ molecules and fragment 1. Thus, according to DFT calculations, the big pores constructed by fragment 1 are considered as the preferential adsorption sites. The conclusion is conflicted with the GCMC results where the small pores composed by fragment 2 are shown as the primary sorption site for $SO_2$ (Figure 2C). The conflict between DFT and GCMC results can be attributed to the restriction of the GCMC method in underestimating the strong interactions using a generic classical force field. Here, it can be suggested that the actual uptake ability of $SO_2$ in ZIF-68 may be even higher than that predicted in this study.

Inducing specific functional groups into the pores of porous materials has been proved to be a useful way to improve the $CO_2$ adsorption ability.[17,36] In our previous study, the effects of functional groups on $CO_2$ adsorption in ZIFs were studied in detail, and the BE of $CO_2$ was significantly enhanced due to the existence of a −$NO_2$ group.[17] Here, the higher BEs of $CO_2$ and $H_2O$ on fragment 2 when comparing to fragment 1 can also be attributed to the enhanced polarized electron densities induced by the −$NO_2$ group. However, for the interaction between $SO_2$ and fragments 1 or 2, comparing to the high BE of $SO_2$ on fragment 1 with no functional group, a much lower BE was obtained on fragment 2 with the −$NO_2$ functional group. It means that the injection of a functional group may be a useful way to inhibit the uptake of $SO_2$ in porous materials. Meanwhile, it is supposed that a porous material with a specific functional group that can improve the $CO_2$ uptake ability and inhibit the uptake of $SO_2$ at the same time will be more applicable for a real postcombustion $CO_2$ capture system.

Additional DFT calculations were performed to investigate the effect of $H_2O$ or $SO_2$ presence on $CO_2$ adsorption in ZIF-68. One $SO_2$ or $H_2O$ molecule was preloaded on its most favorite position of fragments 1 or 2 and optimized, and then, several possible configurations of the $CO_2$ molecule interacting with the $SO_2$ or $H_2O$ molecules on fragments were obtained and optimized, which is available in the Supporting Information.

The brief results of the DFT calculations are illustrated in Figure 6. It is notable that the preloaded $SO_2$ or $H_2O$ molecule does affect the $CO_2$ adsorption on the fragments. On fragment 1, the BE of the first adsorbed $CO_2$ molecule is −9.1 kJ/mol (Table 2), while the BE of the second adsorbed $CO_2$ molecule is −10.9 kJ/mol, as shown in Figure 6a. If the first adsorbed molecule is $H_2O$, the BE of the following adsorbed $CO_2$ molecule raises slightly to −12.2 kJ/mol. If the first adsorbed molecule is $SO_2$, the BE of the following adsorbed $CO_2$ molecule decreases to −8.1 kJ/mol. That is to say, in the big pores constructed by fragment 1, the preloaded $CO_2$ and $H_2O$ molecules are helpful for the following adsorption of $CO_2$, but the preloaded $SO_2$ molecules have negative effects on $CO_2$ adsorption. On fragment 2, the preloaded $H_2O$ molecule also
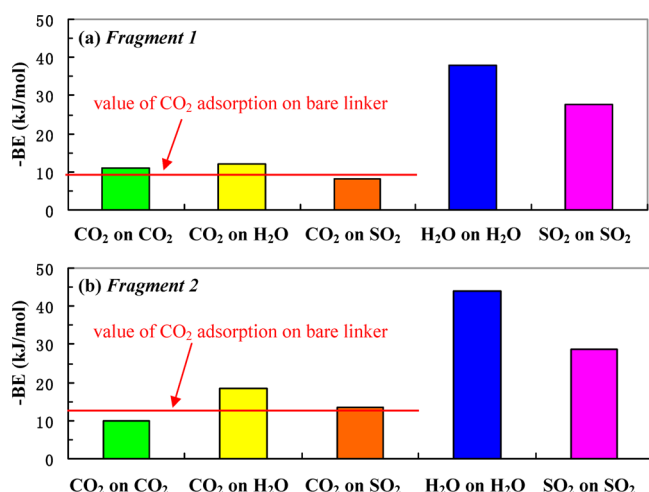
**Figure 6.** BE of $CO_2$ on (a) fragment 1 and (b) fragment 2 with a preloaded gas molecule ($SO_2$ or $H_2O$). BE of $CO_2$ on fragments with preloaded $CO_2$, BE of $H_2O$ on fragments with preloaded $H_2O$, and BE of $SO_2$ on fragments with preloaded $SO_2$ are also presented for comparison. Red line represents the BE of $CO_2$ on bare fragments without any preloaded gas molecule.

significantly enhances the adsorption of $CO_2$ (Figure 6b). However, unlikely on fragment 1, the $CO_2$ adsorption is slightly enhanced by the preloaded $SO_2$ molecule on fragment 2. Despite the fact that the coadsorption of $CO_2$ and $H_2O$ or $SO_2$ is not likely to happen in small pores constructed by fragment 2 due to the steric hindrance effect, it can still be concluded that the role of a polar functional group (such as the $-NO_2$ group in this work) cannot be neglected when evaluating the effects of $SO_2$ and $H_2O$ existence on $CO_2$ adsorption in porous materials.

It is meaningful to give a comprehensive discussion about the effects of $H_2O$ and $SO_2$ on $CO_2$ adsorption in ZIF-68. Here, our simulation results show that the presence of water vapor affects the adsorption of $CO_2$ in MOFs by two opposite ways (positive and negative) in both types of pores, while the case of $SO_2$ is complicated. As shown in Figures 4 and 5b, the $CO_2$ adsorption amount is decreased due to the competitive adsorption with $H_2O$ in the binary and ternary mixtures as the pressure increases. The interaction strength of $CO_2$ in ZIF-68 is significantly weaker than that of $H_2O$ (Tables 1 and 2), making them vulnerable during the competition. The positive effect of $H_2O$ to $CO_2$ adsorption is easy to be observed from the cobinding of $CO_2$ and $H_2O$ calculated using the DFT method (Figure 6): the preloaded $H_2O$ in ZIF-68 will provide additional adsorption sites for $CO_2$. However, the positive effect will not be as significant as what we obtained from the DFT results, because there is another important concern that should not be neglected: the interactions between $H_2O$ and $H_2O$ molecules. The BEs of $H_2O$ on preloaded $H_2O$ fragments are significantly higher than those of $CO_2$ on these preloaded fragments, as shown in Figure 6. That is to say, although additional adsorption sites are provided, these sites may also prefer to be occupied by another $H_2O$ molecule not by a $CO_2$ molecule. But, if the uptake amount of $H_2O$ in ZIF-68 could be carefully controlled in a reasonable content, the $CO_2/N_2$ separation ability are expected to be improved (as observed in Figure 5a), which is very similar to the $CO_2$ adsorption in HKUST-1 with preloaded water.[48] In the case of the effects of $SO_2$, it seems that the preloaded $SO_2$ has either negative (fragment 1) or positive (fragment 2) effects on $CO_2$

adsorption in ZIF-68 from the DFT results shown in Figure 6, which may depend on the functional group used. But overall, the positive effect can be neglected because of the strong interactions between $SO_2$ and the framework as well as among $SO_2$ molecules. Thus, the existence of $SO_2$ inhibits both the $CO_2$ adsorption and the $CO_2/N_2$ separation abilities, as shown in Figure 5.

## 4. CONCLUSIONS

The effects of the presence of water vapor and other gas impurities (such as $SO_2$ and $O_2$) in flue gas on the performance of $CO_2$ adsorption on ZIF-68 were systematically investigated. A hybrid method utilizing both GCMC and DFT calculations was used to give general information of these effects. The results show that the presence of $O_2$ has a negligible effect on $CO_2$ adsorption on ZIF-68. $H_2O$ affects the $CO_2$ adsorption on ZIF-68 in two opposite ways: reduces the $CO_2$ adsorption ability due to the negative effect, but increases the $CO_2/N_2$ separation factor due to the positive effect. However, the presence of $SO_2$ inhibits both the $CO_2$ adsorption and the $CO_2/N_2$ separation abilities of ZIF-68. The results of the simulation will be compared with our experimental results in future work and provide insight into the applications of ZIF materials in realistic $CO_2$ capture systems. Meanwhile, it is also meaningful to investigate the role of different functional groups when evaluating the effects of $H_2O$ and $SO_2$ presence on $CO_2$ adsorption in porous materials in future.

## ■ ASSOCIATED CONTENT

### Ⓢ Supporting Information

Figures showing atomic partial charges of ZIF-68; comparison of simulated and experimental adsorption isotherms of $CO_2$, $N_2$, and $O_2$; uptake amount and isosteric heat of $CO_2$, $N_2$, $O_2$, and $SO_2$ in ZIF-68; uptake amount and isosteric heat of $SO_2$ in ZIF-68 with and without atom charges; selectivity of $CO_2$ from $CO_2/O_2$ mixture; selectivity of $SO_2$ from $SO_2/CO_2$ mixtures; selectivity for $CO_2$ from $CO_2/N_2$; fragments used in this work; possible configurations and binding energies of $H_2O$, $CO_2$, and $SO_2$ on fragment 1; and possible configurations and binding energies of $H_2O$, $CO_2$, and $SO_2$ on fragment 2; and tables showing values for LJ potential parameters; $H_2O$ uptake amount in ZIF-68; $H_2O$ uptake amount without framework charge; $H_2O$ uptake amount without framework and $H_2O$ charge; $H_2O/CO_2$ binary gas adsorption; atomic charge and molecular angle of $CO_2$, $SO_2$, and $H_2O$ before and after adsorbed on fragments 1 and 2. This material is available free of charge via the Internet at http://pubs.acs.org.

## ■ AUTHOR INFORMATION

### Corresponding Author
*Phone: +86 27 87545526; fax: +86 27 87545526; e-mail: liujing27@mail.hust.edu.cn.

### Notes
The authors declare no competing financial interest.

## ■ ACKNOWLEDGMENTS

# ■ REFERENCES

(1) Figueroa, J. D.; Fout, T.; Plasynski, S.; McIvried, H.; Srivastava, R. D. Advances in CO$_2$ Capture Technology—The U.S. Department of Energy's Carbon Sequestration Program. *Int. J. Greenhouse Gas Control* **2008**, *2*, 9−20.

(2) D'Alessandro, D. M.; Smit, B.; Long, J. R. Carbon Dioxide Capture: Prospects for New Materials. *Angew. Chem., Int. Ed.* **2010**, *49*, 6058−6082.

(3) Li, J. R; Sculley, J.; Zhou, H. C. Metal-Organic Frameworks for Separations. *Chem. Rev.* **2012**, *112*, 869−932.

(4) Bhown, A. S.; Freeman, B. C. Analysis and Status of Post-Combustion Carbon Dioxide Capture Technologies. *Environ. Sci. Technol.* **2011**, *45*, 8624−8632.

(5) Wong-Foy, A. G.; Matzger, A. J.; Yaghi, O. M. Exceptional H$_2$ Saturation Uptake in Microporous Metal−Organic Frameworks. *J. Am. Chem. Soc.* **2006**, *128*, 3494−3495.

(6) Banerjee, R.; Phan, A.; Wang, B.; Knobler, C.; Furukawa, H.; O'Keeffe, M.; Yaghi, O. M. High-Throughput Synthesis of Zeolitic Imidazolate Frameworks and Application to CO$_2$ Capture. *Science* **2008**, *319*, 939−943.

(7) Phan, A.; Doonan, C. J.; Uribe-Romo, F. J.; Knobler, C. B.; O'Keeffe, M.; Yaghi, O. M. Synthesis, Structure, and Carbon Dioxide Capture Properties of Zeolitic Imidazolate Frameworks. *Acc. Chem. Res.* **2010**, *43* (1), 58−67.

(8) Park, K. S.; Ni, Z.; Côté, A. P.; Choi, J. Y.; Huang, R.; Uribe-Romo, F. J.; Chae, H. K.; O'Keeffe, M.; Yaghi, O. M. Exceptional Chemical and Thermal Stability of Zeolitic Imidazolate Frameworks. *Proc. Natl. Acad. Sci. U.S.A.* **2006**, *108*, 10186−10191.

(9) Banerjee, R.; Furukawa, H.; Britt, D.; Knobler, C.; O'Keeffe, M.; Yaghi, O. M. Control of Pore Size and Functionality in Isoreticular Zeolitic Imidazolate Frameworks and Their Carbon Dioxide Selective Capture Properties. *J. Am. Chem. Soc.* **2009**, *131*, 3875−3877.

(10) Wang, B.; Côté, A. P.; Furakawa, H.; O'Keeffe, M.; Yaghi, O. M. Colossal Cages in Zeolitic Imidazolate Frameworks as Selective Carbon Dioxide Reservoirs. *Nature* **2008**, *453*, 207−221.

(11) Hayashi, H.; Côte, A. P.; Furakawa, H.; O'Keeffe, M.; Yaghi, O. M. Zeolite A Imidazolate Frameworks. *Nat. Mater.* **2007**, *6*, 501−506.

(12) Liu, D.; Zheng, C.; Yang, Q.; Zhong, C. Understanding the Adsorption and Diffusion of Carbon Dioxide in Zeolitic Imidazolate Frameworks: A Molecular Simulation Study. *J. Phys. Chem. C* **2009**, *113*, 5004−5009.

(13) Liu, B.; Smit, B. Molecular Simulation Studies of Separation of CO$_2$/N$_2$, CO$_2$/CH$_4$, and CH$_4$/N$_2$ by ZIFs. *J. Phys. Chem. C* **2010**, *114*, 8515−8522.

(14) Battisti, A.; Taioli, S.; Garberoglio, G. Zeolitic Imidazolate Frameworks for Separation of Binary Mixtures of CO$_2$, CH$_4$, N$_2$ and H$_2$: A Computer Simulation Investigation. *Microporous Mesoporous Mater.* **2011**, *143*, 46−53.

(15) Sirjoosingh, A.; Alavi, S.; Woo, T. K. Grand-Canonical Monte Carlo and Molecular-Dynamics Simulations of Carbon-Dioxide and Carbon-Monoxide Adsorption in Zeolitic Imidazolate Framework Materials. *J. Phys. Chem. C* **2010**, *114*, 2171−2178.

(16) Bankin, R. B.; Liu, J.; Kulkarni, A. D.; Johnson, J. K. Adsorption and Diffusion of Light Gases in ZIF-68 and ZIF-70: A Simulation Study. *J. Phys. Chem. C* **2009**, *113*, 16906−16914.

(17) Liu, Y.; Liu, J.; Chang, M.; Zheng, C. G. Effect of Functionalized Linker on CO$_2$ Binding in Zeolitic Imidazolate Frameworks: Density Functional Theory Study. *J. Phys. Chem. C* **2012**, *116*, 16985−16991.

(18) Lee, K. B.; Sircar, S. Removal and Recovery of Compressed CO$_2$ from Flue Gas by a Novel Thermal Swing Chemisorption Process. *AIChE J.* **2008**, *54*, 2293−2302.

(19) Sumida, K.; Rogow, D. L.; Mason, J. A.; McDonald, T. M.; Bloch, E. D.; Herm, Z. R.; Bae, T.; Long, J. R. Carbon Dioxide Capture in Metal-Organic Frameworks. *Chem. Rev.* **2012**, *112*, 724−781.

(20) Liu, J.; Wang, Y.; Benin, A. I.; Jakubczak, P.; Willis, R. R.; LeVan, M. D. CO$_2$/H$_2$O Adsorption Equilibrium and Rates on Metal−Organic Frameworks: HKUST-1 and Ni/DOBDC. *Langmuir* **2010**, *26* (17), 14301−14307.

(21) Yu, J.; Balbuena, P. B. Water Effects on Postcombustion CO$_2$ Capture in Mg-MOF-74. *J. Phys. Chem. C* **2013**, *117*, 3383−3388.

(22) Liu, J.; Benin, A. I.; Furtado, A. M. F.; Jakubczak, P.; Willis, R. R.; LeVan, M. D. Selective CO$_2$ Capture from Flue Gas Using Metal−Organic Frameworks——A Fixed Bed Study. *Langmuir* **2011**, *27*, 11451−11456.

(23) Kizzie, A. C.; Wong-Foy, A. G.; Matzger, A. J. Effect of Humidity on the Performance of Microporous Coordination Polymers as Adsorbents for CO$_2$ Capture. *Langmuir* **2011**, *27*, 6368−6373.

(24) Yazaydin, A. Ö.; Benin, A. I.; Faheem, S. A.; Jakubczak, P.; Low, J. J.; Willis, R. R.; Snurr, R. Q. Enhanced CO$_2$ Adsorption in Metal-Organic Frameworks via Occupation of Open-Metal Sites by Coordinated Water Molecules. *Chem. Mater.* **2009**, *21*, 1425−1430.

(25) Huang, H.; Zhang, W.; Liu, D.; Zhong, C. Understanding the Effect of Trace Amount of Water on CO$_2$ Capture in Natural Gas Upgrading in Metal−Organic Frameworks: A Molecular Simulation Study. *Ind. Eng. Chem. Res.* **2012**, *51* (31), 10031−10038.

(26) Ding, L.; Yazaydin, A. Ö. How Well Do Metal−Organic Frameworks Tolerate Flue Gas Impurities? *J. Phys. Chem. C* **2012**, *116* (43), 22987−22991.

(27) Wang, W.; Peng, X.; Cao, D. Capture of Trace Sulfur Gases from Binary Mixtures by Single-Walled Carbon Nanotube Arrays: A Molecular Simulation Study. *Environ. Sci. Technol.* **2011**, *45*, 4832−4838.

(28) Thallapally, P. K.; Motkuri, R. K.; Fernandez, C. A.; McGrail, B. P.; Behrooz, G. S. Prussian Blue Analogues for CO$_2$ and SO$_2$ Capture and Separation Applications. *Inorg. Chem.* **2010**, *49*, 4909−4915.

(29) Ding, L.; Yazaydin, A. Ö. The Effect of SO$_2$ on CO$_2$ Capture in Zeolitic Imidazolate Frameworks. *Phys. Chem. Chem. Phys.* **2013**, *15*, 11856−11861.

(30) Casewit, C. J.; Colwell, K. S.; Rappe, A. K. Application of a Universal Force Field to Organic Molecules. *J. Am. Chem. Soc.* **1992**, *114*, 10035−10046.

(31) Rappé, A. K.; Casewit, C. J.; Colwell, K. S.; Goddard, W. A., III; Skiff, W. M. UFF, a Full Periodic Table Force Field for Molecular Mechanics and Molecular Dynamics Simulations. *J. Am. Chem. Soc.* **1992**, *114*, 10024−10035.

(32) Ohkubo, T.; Miyawaki, J.; Kaneko, K.; Ryoo, R.; Seaton, N. A. Adsorption Properties of Templated Mesoporous Carbon (CMK-1) for Nitrogen and Supercritical Methane − Experiment and GCMC Simulation. *J. Phys. Chem. B* **2002**, *106* (25), 6523−6528.

(33) Hirotani, A.; Mizukami, K.; Miura, R.; Takaba, H.; Miya, T.; Fahmi, A.; Stirling, A.; Kubo, M.; Miyamoto, A. Grand Canonical Monte Carlo Simulation of the Adsorption of CO$_2$ on Silicalite and NaZSM-5. *Appl. Surf. Sci.* **1997**, *120*, 81−84.

(34) Maitland, G. C.; Rigby, M.; Smith, E. B.; Wakeham, W. A. *Intermolecular Forces: Their Origin and Determination*; Clarendon Press: Oxford, U.K., 1981.

(35) Accelrys Software Inc. *Materials Studio Release Notes*, Release 4.4; Accelrys Software Inc.: San Diego, CA, 2008.

(36) Liu, Y.; Liu, J.; Chang, M.; Zheng, C. G. Theoretical Studies of CO$_2$ Adsorption Mechanism on Linkers of Metal-Organic Frameworks. *Fuel* **2012**, *95*, 521−527.

(37) Delley, B. From Molecules to Solids with the DMol$^3$ Approach. *J. Chem. Phys.* **2000**, *113*, 7756−7764.

(38) Perdew, J. P.; Wang, Y. Accurate and Simple Analytic Representation of the Electron-Gas Correlation Energy. *Phys. Rev. B* **1992**, *45*, 13244−13249.

(39) Ramsahye, N. A.; Maurin, G.; Bourrelly, S.; Llewellyn, P. L.; Serre, C.; Loiseau, T.; Devic, T.; Férey, G. Probing the Adsorption Sites for CO$_2$ in Metal Organic Frameworks Materials MIL-53 (Al, Cr) and MIL-47 (V) by Density Functional Theory. *J. Phys. Chem. C* **2008**, *112*, 514−520.

(40) Delley, B. Hardness Conserving Semilocal Pseudopotentials. *Phys. Rev. B* **2002**, *66*, 155125−155134.

(41) Torrisi, A.; Mellot-Draznieks, C.; Bell, R. G. Impact of Ligands on CO$_2$ Adsorption in Metal-Organic Frameworks: First Principles Study of the Interaction of CO$_2$ with Functionalized Benzenes.II.

Effect of Polar and Acidic Substituents. *J. Chem. Phys.* **2010**, *132*, 044705.

(42) Torrisi, A.; Mellot-Draznieks, C.; Bell, R. G. Impact of Ligands on $CO_2$ Adsorption in Metal-Organic Frameworks: First Principles Study of the Interaction of $CO_2$ with Functionalized Benzenes.I. Inductive Effects on the Aromatic Ring. *J. Chem. Phys.* **2009**, *130*, 194703.

(43) Torrisi, A.; Bell, R. G.; Mellot-Draznieks, C. Predicting the Impact of Functionalized Ligands on $CO_2$ Adsorption in MOFs: A Combined DFT and Grand Canonical Monte Carlo Study. *Microporous Mesoporous Mater.* **2013**, *168*, 225−238.

(44) Vitillo, J. G.; Regli, L.; Chavan, S.; Ricchiardi, G.; Spoto, G.; Dietzel, P. D. C.; Bordiga, S.; Zecchina, A. Role of Exposed Metal Sites in Hydrogen Storage in MOFs. *J. Am. Chem. Soc.* **2008**, *130*, 8386−8396.

(45) Suri, M.; Dornfeld, M.; Ganz, E. Calculation of Hydrogen Storage Capacity of Metal-Organic and Covalent-Organic Frameworks by Spillover. *J. Chem. Phys.* **2009**, *131*, 174703.

(46) Srepusharawoot, P.; Araújo, C. M.; Blomqvist, A.; Scheicher, R. H.; Ahuja, R. A Comparative Investigation of $H_2$ Adsorption Strength in Cd- and Zn-Based Metal Organic Framework-5. *J. Chem. Phys.* **2008**, *129*, 164104.

(47) Lee, T. B.; Kim, D.; Jung, D. H.; Choi, S. B.; Yoon, J. H.; Kim, J.; Choi, K.; Choi, S. H. Understanding the Mechanism of Hydrogen Adsorption into Metal Organic Frameworks. *Catal. Today* **2007**, *120*, 330−335.

(48) Yazaydin, A. Ö.; Benin, A. I.; Faheem, S. A.; Jakubczak, P.; Low, J. L.; Willis, R. R.; Snurr, R. Q. Enhanced $CO_2$ Adsorption in Metal-Organic Frameworks via Occupation of Open-Metal Sites by Coordinated Water Molecules. *Chem. Mater.* **2009**, *21*, 1425−1430.